ELSEVIER

International Journal of Mass Spectrometry 219 (2002) 485–495

International Journal of Mass Spectrometry

www.elsevier.com/locate/ijms

Photodetachment of $FSi(OMe)_4^-$ and $FGe(OMe)_4^-$ anions: an experimental and theoretical study of gas-phase hypervalent Si and Ge species

Luciano A. Xavier[a], Nelson H. Morgon[b], Jair J. Menegon[a], José M. Riveros[a,*]

[a] *Instituto de Química, Universidade de São Paulo, Av. Lineu Prestes 748, Cidade Universitária, São Paulo, CEP 05508-900, Brazil*
[b] *Instituto de Química, Universidade Estadual de Campinas (UNICAMP), Caixa Postal 6154, Campinas, SP, CEP 13083-970, Brazil*

Received 16 January 2002; accepted 29 March 2002

Dedicated to Yannick Hoppilliard for her contribution to mass spectrometry in France and with very fond memories of the memorable International Mass Spectrometry Conference that she organized in Bordeaux.

Abstract

The structure and thermochemistry of the hypervalent $FSi(OMe)_4^-$, $FGe(OMe)_4^-$ and $FGe(H)(OMe)_3^-$ anions have been investigated by a combination of photodetachment spectroscopy and ab initio calculations. All three of these anions undergo photodetachment at wavelengths between 266 and 285 nm but not at 355 nm. The data suggest that the observed photodetachment process for these ions is a one-photon process leading to dissociation of a MeO group for the first two anions, and presumably dissociation of a H atom in the last case. Theoretical calculations are consistent with these observations and predict a fluoride binding energy of 47.5 kcal mol^{-1} and a methoxide binding energy of 52 kcal mol^{-1} in $FSi(OMe)_4^-$. The most stable structure for $FSi(OMe)_4^-$ is predicted to be a trigonal bipyramid with the fluorine occupying an axial position. This is similar to what has been found for the corresponding $Ge(OMe)_4$ species. These results, the gas-phase chemical behavior of these anions, and the calculated charge distribution are consistent with anions in which a high degree of covalent bonding exists between the electronegative ligand and the central Si or Ge atom. (Int J Mass Spectrom 219 (2002) 485–495)

Keywords: Hypervalent anions of Si and Ge; Photodetachment; Fluoride affinity; Computational Si chemistry

1. Introduction

Hypervalent silicon species have attracted considerable interest in the last decades because of their distinct reactivity and because they are important intermediates in a wide range of nucleophilic reactions. Much of our knowledge about these species is due to the pioneering work of Corriu and coworkers that has been brilliantly described in a very comprehensive review [1]. In recent years, a growing number of these species have been characterized by NMR and X-ray crystallography as they become amenable for structural determination in condensed phases [2]. Considerably less is known about the corresponding Ge systems even though nucleophilic type reactions are also assumed to proceed through hypervalent Ge intermediates [3]. In the gas phase, several pentacoordinated silicon anions have been identified as products of ion/molecule reactions between simple nucleophiles and organosilanes [4–6] and their struc-

* Corresponding author. E-mail: jmrnigra@quim.iq.usp.br

1387-3806/02/$ – see front matter
PII S1387-3806(02)00702-9

ture and stability have been investigated by ab initio calculations [7]. Our group has been concerned for some years with the gas-phase ion chemistry of silicon alkoxides, $Si(OR)_4$, [8–10] and germanium alkoxides, $Ge(OR)_4$, [11,12] in order to elucidate the mechanism of nucleophilic reactions that are of paramount importance in the preparation of important silicon [13] and Ge [14] materials by sol–gel processes.

Several of the anionic pentacoordinated species obtained in our previous studies are particularly interesting because they are directly related to chemical problems in condensed phases. For example, $Si(OMe)_5^-$, the main product of the ion/molecule reaction between MeO^- and $Si(OMe)_4^-$ [8], has been used as a model to establish the importance of pentacoordinated intermediates in reactions related to hydrolysis and gel formation [15]. Likewise, the $FSi(OMe)_4^-$ ion previously observed in the gas-phase [8] is considered to be the relevant species in the activation of Si–O bonds catalyzed by F^- [16]. While some structural information is available for pentacoordinated Si anions containing fluorine [17–19], little is still known regarding the enegetics of these species, and in particularly those involving the Si and Ge alkoxides.

The present report describes results obtained from photodetachment experiments carried out in our FT-ICR spectrometer with the objective to establish structural and energetic features of $FSi(OMe)_4^-$, $FGe(OMe)_4^-$ and related Ge anions. Electron photodetachment is well established as a technique for determining the electron affinity of anions [20] and can provide valuable information regarding the structure of complex ions [21]. In a previous paper [22], threshold photodetachment experiments in conjunction with ab initio calculations [23] were used to determine the binding energies of complex ions such as $X^-(HOR)$ for X = F, Cl, Br, I. In the present case, ab initio calculations are reported for the $FSi(OMe)_4^-$ system to complement our experimental observations.

2. Experimental

Experiments were carried out in our FT-ICR spectrometer interfaced to an IonSpec Omega Fourier Transform Data System. The general characteristics of our spectrometer have been illustrated in recent publications from these laboratories [8,9,12]. It operates with an electromagnet usually set at 1.0 T and uses a $\sim$15.6 cm^3 cubic cell with center holes on both transmitter plates to allow for laser light to go through the cell. The vacuum can holding the ICR cell is provided with two sapphire windows acting as an entry and exit port for laser radiation.

F^- ions were typically generated from NF_3 (Pennwalt Ozark Mahoning) by dissociative electron attachment at 3.5 eV with a 40 ms electron beam pulse. The partial pressure of NF_3 was maintained in the vicinity of 2.0×10^{-8} Torr. Typical trapping voltages for these experiments were −1.9 V. In most cases, a radio-frequency field of $\sim$7 MHz was applied to one of the trapping plates during 100 ms to remove trapped thermal electrons from the cell. Tetramethoxysilane, $Si(OMe)_4$, and germanium methoxide, $Ge(OMe)_4$, were obtained from Aldrich, and samples were repeatedly distilled under vacuum prior to introduction in the cell. This procedure was essential to minimize the amount of methanol resulting from hydrolysis of these compounds.

Ion/molecule reactions between F^- and $Ge(OMe)_4$, or $Si(OMe)_4$, were studied as before [8,9,12] by isolating the ions of interest with a combination of radio-frequency pulses to eject all unwanted ions from the ICR cell. Ions were typically isolated 1 s after the ionization pulse to allow for collisional and radiative relaxation.

Photodetachment experiments were carried out using a Spectra Physics Nd:YAG laser model GCR-3. In some experiments, the second harmonic of this laser at 532 nm was used to pump a Spectra Physics PDL-3 Dye Laser. The output of the dye laser was doubled using an INRAD dye doubler provided with an autotracker and a UV harmonic separator. Since this laser operates best at a 10 Hz repetition rate, the timing sequence of the FT experiment was modified according to a procedure developed in these laboratories [24]: (a) a pulse from the oscillator output of the Nd:YAG laser was used to trigger externally the time base of the Fourier Transform Data System; (b) with the

flashlamps operating at 10 Hz, the Q-switch of the laser was gated from a pulse originating from the Data System through a pulse generator at the appropriate time as controlled on a two-channel oscilloscope. The laser beam was guided to the cell through a set of prisms and an iris and no focusing was used for these experiments. The energy of the laser was measured with an Ophir Laserstar energy meter prior to the first 90° bending prism, and thus the energy measured is substantially higher than that reaching the center of the ICR cell.

The fractional decrease (FD) of the intensity of the ion undergoing photodetachment was obtained from the FT-ICR spectra recorded with and without laser irradiation.

3. Photodetachment experiments of $FSi(OMe)_4^-$

The ion/molecule reaction between F^- and $Si(OMe)_4$ has been previously described [4,8]. $FSi(OMe)_4^-$ ($m/z = 171$) becomes the most important reaction product with thermalized F^-. Initial experiments using either the second (532 nm) or third harmonic (366 nm) of the Nd:YAG laser revealed that no photodissociation or photodetachment occurs at these wavelengths. While even crude estimates of the energetics of the possible photodetachment processes yield threshold values well below 355 nm, these experiments were important to establish an experimental protocol and eliminate artifacts originating from the laser hitting any of the walls of the cell. A very different situation is observed when the ions are irradiated with the fourth harmonic of the Nd:YAG laser at 266 nm. At this wavelength, a substantial decrease in intensity is observed in the FT-ICR spectrum for the isolated $FSi(OMe)_4^-$ ion. Since no photodissociation product was detected, this decrease in intensity was interpreted as the result of a photodetachment process. No attempt was made to use CCl_4 as a low energy electron scavenger to yield Cl^- ions because of our previous experience with the ease of spurious appearance of Cl^- ions when using CCl_4.

Photodetachment was also observed up to 285 nm by doubling the output of the dye laser with a suitable dye. Unfortunately, it was not possible to go to higher wavelengths because our dye laser requires a delay line that is presently unavailable in our laboratories.

Unlike some of the recent and very elegant photodetachment–photofragment coincidence spectroscopy experiments where both electron and neutral fragments are identified [25], the interpretation of our experiment requires some speculation regarding the nature of the neutral photoproduct(s). The first alternative is the possibility that photodetachment of $FSi(OMe)_4^-$ could yield the putative neutral radical $[FSi(OMe)_4]$ as:

$$FSi(OMe)_4^- + h\nu \rightarrow [FSi(OMe)_4]^\bullet + e^- \quad (1)$$

At present, there is considerable doubt as to whether such a hypervalent Si radical is a stable species. Theoretical calculations [26,27] on the related SiF_5 radical are inconclusive as depending on the level of calculation SiF_5 is predicted either to be unstable or to have very low binding energies (<10 kcal mol^{-1}). Furthermore, no experimental evidence is available for the existence of these species in the gas phase or in condensed phases. Thus, we have assumed that the most likely situation in our experiment corresponds to a dissociative photodetachment that could involve a short-lived $[FSi(OMe)_4]^\bullet$ species. Two main possibilities can be considered for a dissociative photodetachment process:

(a) Dissociation by Si–F cleavage:

$$FSi(OMe)_4^- + h\nu \rightarrow F + Si(OMe)_4 + e^- \quad (2)$$

If this is the case, the energetics of the process can be equated in terms of the fluoride dissociation energy in $FSi(OMe)_4^-$, here defined as $D[F^- \cdots Si(OMe)_4]$, and the electron affinity (EA) of F

$$h\nu_{laser} > D[F^- \cdots Si(OMe)_4] + EA(F)$$

(b) Dissociation by Si–OMe cleavage:

$$FSi(OMe)_4^- + h\nu \rightarrow MeO + FSi(OMe)_3 + e^- \quad (3)$$

If this is the case, and by analogy with reaction (2), the energetics can be equated in terms of the methoxide dissociation energy in $FSi(OMe)_4^-$, here defined as $D[MeO^- \cdots FSi(OMe)_3]$, and the EA of MeO

$$h\nu_{laser} > D[MeO^- \cdots FSi(OMe)_3] + EA(MeO^\bullet)$$

Our earlier ab initio calculations [9] explored the $FSi(OMe)_4^-$ ion only superficially and not at a very high level of theory. From these early calculations, it was unclear whether either of the two dissociative photodetachment processes indicated above could occur even at 266 nm. Therefore, it became important to establish whether the observed process was a one- or two-photon process. Photodetachment by a two-photon process through a bound excited electronic state has been previously observed for a number of polycyano compounds [28], and the proposal was advanced that low lying excited states for anions could be observed in organometallic complexes as a result of charge transfer bands. For a two-photon process, the FD of ions due to photodetachment can be represented in the simplest case by

$$FD = 1 - \exp\left[\frac{-\sigma_1\sigma_2 I^2 t}{k + \sigma_2 I}\right] \quad (4)$$

where I represents the intensity of the incident radiation, σ_1 and σ_2 the cross section for the first and second absorption, t the pulse width of the laser (~8 ns) and k the relaxation rate constant for all processes. This expression clearly suggests that at low laser intensities, there should be a non-linear behavior with intensity.

Fig. 1 shows the FD observed for $FSi(OMe)_4^-$ as a function of relative laser energy. (The actual laser energy in the center of the cell is difficult to determine and may be considerably less than that measured at

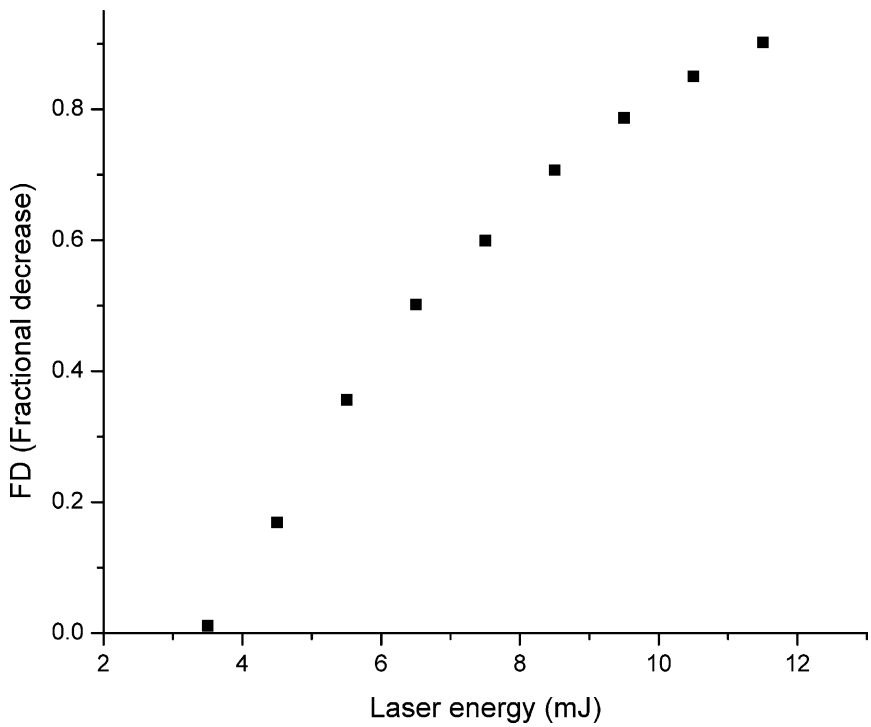

Fig. 1. Fractional decrease of the intensity of the $FSi(OMe)_4^-$ ion in the FT-ICR spectrum as a function of the laser energy measured at the output of the laser. Laser energy in the center of the cell is unknown but it is certainly much lower than that measured by the energy meter.

the output of the laser.)

$$\mathrm{FD} = \frac{I_0 - I_{\mathrm{laser}}}{I_0} \quad (5)$$

From this graph, we find no indication that the observed photodetachment process can be ascribed to a two-photon process since FD is essentially linear at the lower laser energies. At very high percentages of photodetachment, the observed curvature in the graph is not unusual in this type of experiment and may be due to the fact that not all the ions detected by FT-ICR are in the cell within the diameter of the laser beam in the 8 ns pulse.

From the photodetachment observed at 285 nm, and using the known value of 3.40 eV [29] for the electron affinity of F, we can rule out process (1) since that would imply a $D[F^- \cdots Si(OMe)_4]$ less than 22 kcal mol^{-1}. This value is much too low compared with the fluoride affinity of organosilanes that are typically in the 40 kcal mol^{-1} range or higher [5,30]. On the other hand, considering the electron affinity of the MeO radical, namely 1.57 eV [31], the fact that photodetachment is observed up to 285 nm but not at 355 nm suggests that process (2) may be possible provided that $44\ \mathrm{kcal\ mol^{-1}} \leq D[MeO^- \cdots FSi(OMe)_3] < 64\ \mathrm{kcal\ mol^{-1}}$. This is a reasonable range for methoxide affinities event though no data are available for organosilanes.

4. Theoretical investigation of the $FSi(OMe)_4^-$ anion

The results obtained from the photodetachment experiments prompted us to investigate the energetics of this ion by high level ab initio calculations. We have previously described the use of the generator coordinate method (GCM) [32,33] to develop appropriate basis sets for Si and Ge species [9,12]. Our procedure makes use of an effective core potential, ECP [34], for the internal electrons while retaining a high quality criterion for treating the valence electrons of neutrals and anionic species [35]. This methodology has been shown to yield excellent values for the thermochemistry of anions [36] at a considerably reduced computational cost due to the use of an effective core potential.

In the present case, the computational procedure involved the following steps:

(i) obtaining the valence basis sets from the 7s, 5p and 1d set of functions adapted to the pseudopotential (ECP) of Stevens and coworkers [34] for C, O, F and Si, and 4s/1p for H;
(ii) contraction of the basis sets obtained in (i) with reoptimization of the exponents of the primitive functions (4 1 1 1/3 1 1/1 functions for C, O, F and Ge, and 3 1 1/1 for H) leading to what we define as GCM/ECP basis set;
(iii) addition of diffuse functions (s and p type) to correct the valence region, and additional polarization functions (p for H, and d and f for C, F, O, and Si), for more refined energy calculations. This results in a (4 1 1 1 1/3 1 1 1/1 1/1 1) set for C, O, F and Si, and a (3 1 1 1/1 1) set for H and is referred to as our (GCM+/ECP) basis set.

Molecular geometries were initially optimized with the basis set outlined in step (ii) and vibrational frequencies calculated at the HF/(GCM/ECP) level. The zero-point energies (ZPE) obtained from these frequencies were scaled by 0.8929 in the final energy calculations. Using the structures obtained at the HF/(GCM/ECP) level and the calculated force constants, a new geometry optimization was performed at the MP2/(GCM/ECP) level resulting in a lower computational cost for calculating molecular geometries at MP2 level. The more refined energy calculations, namely E(MP2/GCM+/ECP), were then carried out with the latter geometry.

All calculations were carried out using the Gaussian 94 suite of programs [37].

5. Results of theoretical calculations

Calculations on the $FSi(OMe)_4^-$ system reveal two different isomeric species corresponding to trigonal bipyramid structures with F either in an axial

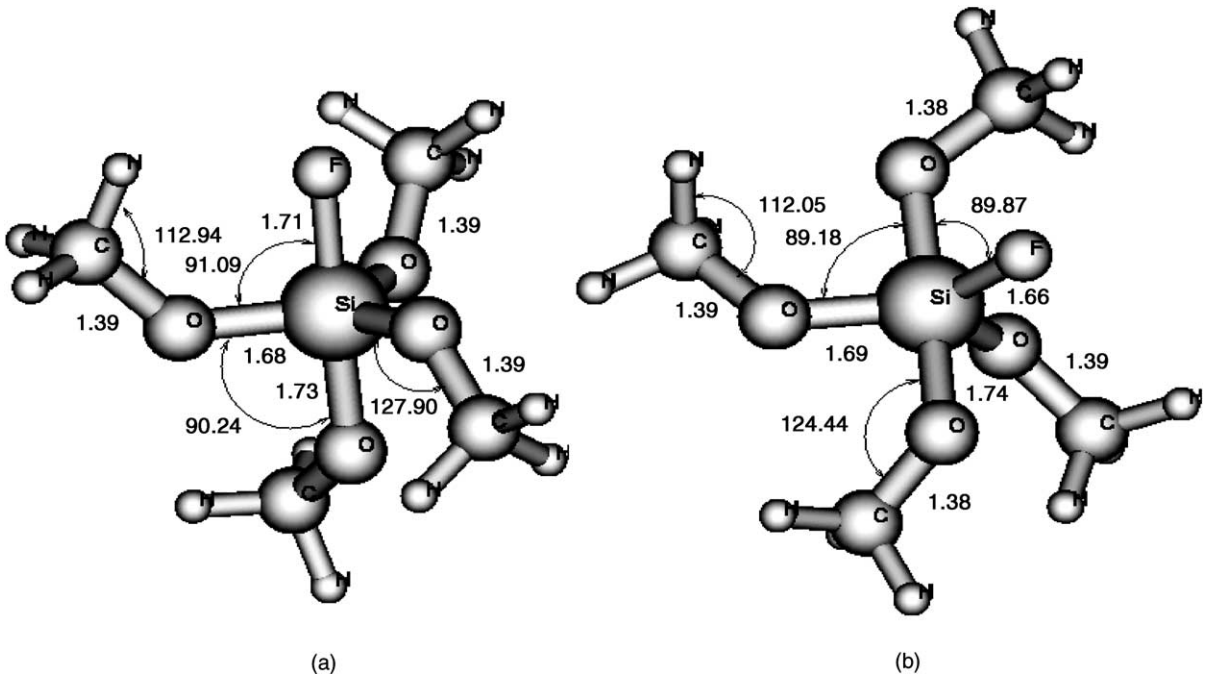

Fig. 2. Optimized geometries for the most stable isomeric species of $FSi(OMe)_4^-$ with (a) the fluorine in an axial position of a trigonal bipyramid, and (b) the fluorine occupying an equatorial position in an trigonal bipyramid.

or equatorial position. The optimized structures for these two isomers are shown in Fig. 2. Structure (a), axial $FSi(OMe)_4^-$, with the fluorine occupying the axial position is more stable than structure (b), equat $FSi(OMe)_4^-$, by 3.2 kcal mol^{-1} as shown in Table 1. This preference for the axial position for an electronegative fifth ligand is similar to what has been found in other computational studies of pentacoordinated Si compounds [38]. The calculated geometries also reveal that the axial bond lengths are somewhat longer than the equatorial bond distances but the differences are not large. This is in line with the view that Si attached to a large number of electronegative groups leads to very tight hypervalent Si species [2c].

The calculated energies for the relevant species involved in processes (1) and (2), and these two isomeric pentaacoordinated species are given in Table 1. As an initial test of our calculated values, the proton

Table 1
Calculated energies at different levels using the basis set developed by the generator coordinate method with geometries optimized at the MP2 level (a.u.), and zero-point energies (ZPE, kcal mol^{-1}) for the neutrals and anionic species relevant to the photodetachment process of $FSi(OMe)_4^-$

System	E(MP2/ECP/GCM)	E(MP2/ECP/GCM+)	ZPE HF/ECP/GCM	E(MP2/ECP/MCG+) + ZPE (a.u.)
F^-	−24.114003	−24.186809		−24.186809
MeO^-	−23.289877	−23.350523	23.45	−23.317149
$FSi(OMe)_3$	−98.186367	−98.393233	86.92	−98.269545
$Si(OMe)_4$	−97.352128	−97.568769	113.37	−97.407456
$FSi(OMe)_4^-$ (ax)	−121.575389	−121.832684	114.41	−121.669888
$FSi(OMe)_4^-$ (eq)	−121.570604	−121.827427	114.29	−121.664805

Table 2
Comparative values of calculated proton affinities for F^- and MeO^- (kcal mol^{-1}) using our GCM methodology and other common methods

	MP2/GCM+/ECP// MP2/(GCM/ECP)	MP2/6-31+G(2df,p)// MP2/6-31+G*	B3LYP/6-31+G(2df,p)// B3LYP/6-31+G*	Experimental
F^-	369.3	367.8	369.3	371.3
MeO^-	380.3	381.2	380.9	382

Table 3
Calculated fluoride and methoxide dissociation energies (kcal mol^{-1})[a] at 0 K for $FSi(OMe)_4^-$

	$D[F^- \cdots Si(OMe)_4]^-$	$D[MeO^- \cdots FSi(OMe)_3]^-$
Axial $FSi(OMe)_4^-$ [b]	47.5	52.2
Equatorial $FSi(OMe)_4^-$ [c]	44.3	49.0

[a] Zero-point energies were adjusted by 0.89 to correct for the calculated vibrational frequencies.
[b] This ion is a trigonal bipyramid with the F occupying an axial position.
[c] This ion is a trigonal bipyramid with the F occupying an equatorial position.

affinities of F^- and MeO^- were calculated using our methodology and compared to those obtained by an all electron MP2/6-31+G(2df,p)//MP2/6-31+G* and by B3LYP/6-31+G(2df,p)//B3LYP/6-31+G*. The results shown in Table 2 reveal that our method yields reliable values of proton affinities when compared with experimental values and with other methods.

The calculated F^- and MeO^- binding energies obtained from these calculations are listed in Table 3 for both isomers and refer to 0 K. It is noticeable that the methoxide binding energy in $FSi(OMe)_4^-$ is higher than the corresponding fluoride binding energy. From these results, we can estimate that the adiabatic threshold for photodetachment according to process (1) should be around 227 nm, and for process (2) around 323 nm. Thus, the theoretical calculations clearly predict that the dissociative photodetachment process in $FSi(OMe)_4^-$ should proceed according to process (3).

Another important consideration in the analysis of these hypervalent species is the charge distribution in the anion. While the interpretation of atomic charges and how to calculate them is a matter of considerable controversy, we have listed in Table 4 the atomic charges calculated for $FSi(OMe)_4^-$ using Mulliken's population analysis as our simplest model. The values in Table 4 suggest that the negative charge is highly delocalized among the oxygens and fluorines and that this ion cannot be simply represented as an adduct. This view is strongly supported by the chemical behavior of this pentacoordinated complex as discussed below.

Table 4
Calculated atomic charges obtained by Mulliken's population analysis

Atom	Mulliken charge ax-$FSi(OMe)_4^-$ [a]	Mulliken charge eq-$FSi(OMe)_4^-$ [b]
Si	1.19	1.21
F	−0.56	−0.52
Equatorial O	−0.49 to −0.52	−0.51
Axial O	−0.51	−0.53
C	0.09–0.13	0.10–0.14
H	−0.01 to 0.04	−0.02 to 0

[a] This ion is a trigonal bipyramid with the H occupying an axial position.
[b] This ion is a trigonal bipyramid with the H occupying an equatorial position.

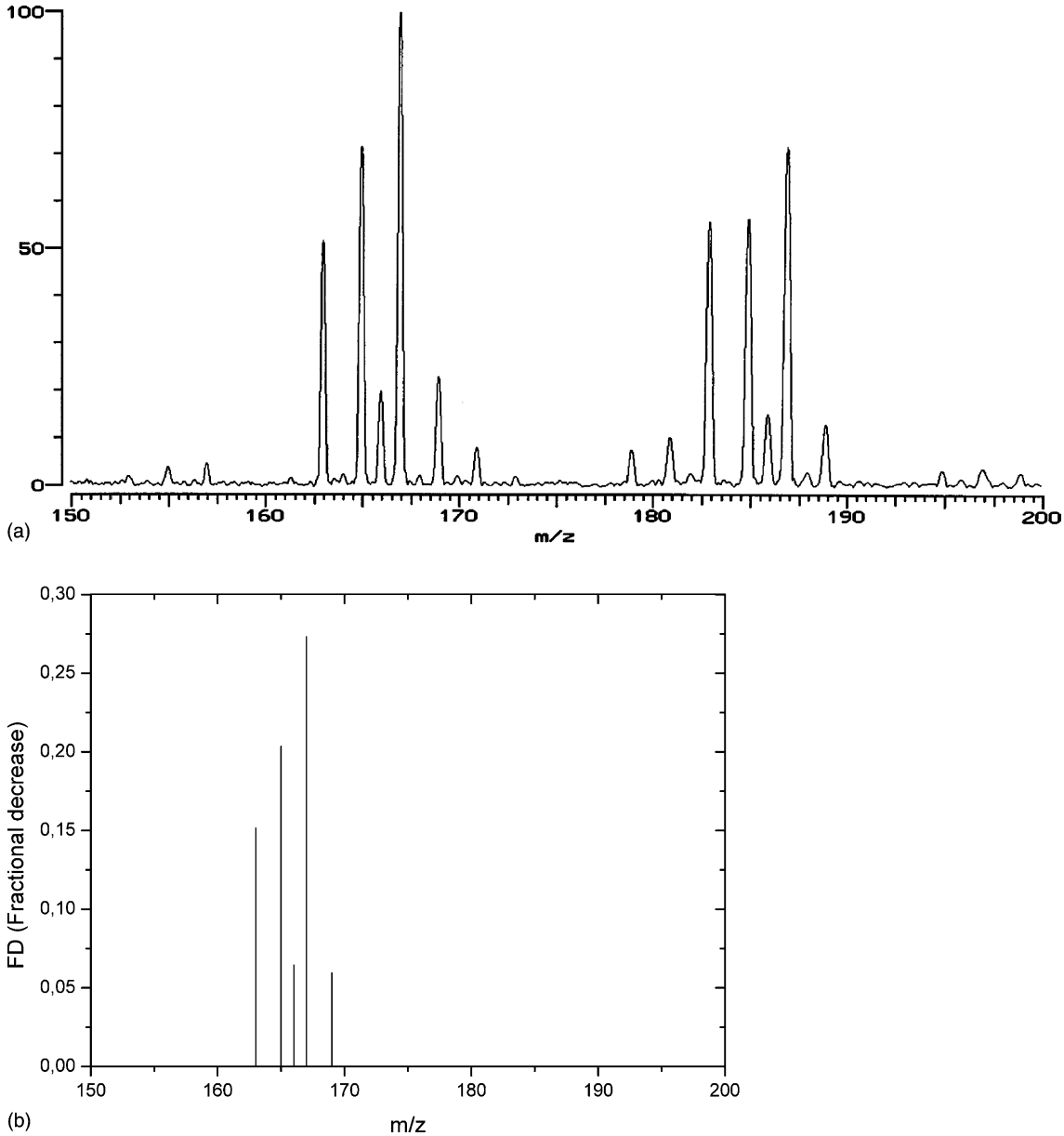

Fig. 3. (a) FT-ICR spectrum of isolated ion/molecule reaction products of $F^- + Ge(OMe)_4$ in the range of $m/z = 150$–200. (b) Fractional decrease of ion intensities (between $m/z = 150$ and 200) obtained after irradiation with the Nd:YAG laser set at 355 nm. For comparison purposes, ions between $m/z = 150$ and 200 were not ejected prior to laser irradiation. This graph reveals that only the peaks corresponding to $Ge(OMe)_3^-$ (main isotopic species at $m/z = 167$) are affected by the laser. Notice that $FGe(H)(OMe)_3^-$ (base peak at $m/z = 187$) is not changed by the laser irradiation. The isotopic distribution of the latter ion is affected by the contribution due to the minor product $(MeO)_3GeO^-$ (main isotopic species at $m/z = 183$).

6. Photodetachment of Ge-containing anions

The ion/molecule reaction of F^- with $Ge(OMe)_4$ has been shown [11] to yield primarily $FGe(OMe)_4^-$ (the main product), $Ge(OMe)_3^-$ and $FGe(H)(OMe)_3^-$, as well as other minor products.

The photodetachment characteristics of these ions were also studied following the procedure outlined above. At 355 nm, photodetachment is observed only for $Ge(OMe)_3^-$ as shown in Fig. 3. This observation is consistent with our estimate that the electron affinity of $Ge(OMe)_3^-$ is 2.32 eV [39]. On the other hand, and similar to what has been described for the corresponding $FSi(OMe)_4^-$, photodetachment for $FGe(OMe)_4^-$, $FGe(H)(OMe)_3^-$ (most intense isotopic species at $m/z = 187$) and $Ge(OMe)_3^-$ is observed at 266 nm and up to 285 nm.

By analogy with $FSi(OMe)_4^-$, the photodetachment process observed in $FGe(OMe)_4^-$ is assumed to be a dissociative process. Recent theoretical calculations [40] on the related hypervalent GeF_5 radical are inconclusive as different DFT methods predict this species either to be slightly bound or to be a transition state. Thus, the process above threshold is best described as follows:

$$FGe(OMe)_4^- + h\nu\,(266\,\text{nm}) \rightarrow MeO + FGe(OMe)_3 + e^- \quad (6)$$

In our previous calculation on Ge systems [12], the fluoride affinity of the model $Ge(OH)_4$ substrate was predicted to be of the order of 60 kcal mol^{-1}. This value clearly eliminates the possibility of fluorine elimination in the photodetachment process at these wavelengths.

On the other hand, the results with the other pentacoordinated adduct, $FGe(H)(OMe)_3^-$, are very interesting. Hydrogen is expected to be more stable in an equatorial position of the trigonal bipyramid as determined from our calculations on the $HGe(OH)_4^-$ model system [12] in line with the view that the more electronegative ligands in a trigonal bipyramid structure prefer the axial position [38]. From the known value of 0.754 eV for the electron affinity of H [41], and using similar arguments as those advanced in Eqs. (2) and (3) we can conclude from the lack of photodetachment at 355 nm that either

(a) $D[H^- \cdots FGe(OMe)_3] \geq 63$ kcal mol^{-1} since

$$FGe(H)(OMe)_3^- + h\nu\,(355\,\text{nm}) \rightarrow \text{no photodetachment observed} \quad (7)$$

or

(b) $D[MeO^- \cdots FGe(H)(OMe)_2] \geq 44$ kcal mol^{-1} since

$$FGe(H)(OMe)_3^- + h\nu\,(355\,\text{nm}) \rightarrow \text{no photodetachment observed.} \quad (8)$$

These conclusions are conservative because it is unclear whether the actual threshold for photodetachment can be determined for these hypervalent species. Since the neutral surface is assumed to be of a dissociative character, the adiabatic transition necessary to establish true lower values to the dissociation energies may be difficult because of unfavorable Franck–Condon factors.

The second alternative (Eq. (8)) is consistent with the observation on the Si system but the first conclusion needs careful consideration. Our calculation on the $HGe(OH)_4^-$ model system [12] estimated the hydride affinity of $Ge(OH)_4$ (from an equatorial position) to be about 60 kcal mol^{-1}. This is close to the low limit value established by Eq. (7).

Our previous calculation on the prototype $FGe(OH)_4^-$ anion [12] reveals strong similarities with the present calculations on the $FSi(OMe)_4^-$. In both cases, an axial position is preferred for the fluorine atom and the negative charge is predicted to be evenly distributed between fluorine and the oxygen atoms following a Mulliken's population analysis.

7. Conclusions

The experimental data and the theoretical calculations presented in this paper clearly point out that hypervalent species like the anion $FSi(OMe)_4^-$ and $FGe(OMe)_4^-$ are tightly bound species with high

degree of covalency. Thus, dissociation energies for releasing F^-, MeO^-, or even H^- in the case of $FGe(H)(OMe)_3^-$ are very high compared to the usual adducts observed in gas-phase ion chemistry.

The chemical behavior of these species also points towards the stability of these species. Experiments carried out with F^- and mixtures of $Si(OMe)_4$ and $Ge(OMe)_4$ revealed that $FGe(OMe)_4^-$ is unreactive towards $Si(OMe)_4$, and $FSi(OMe)_4^-$ ions are unreactive towards $Ge(OMe)_4$. Thus, there is no tendency for fluoride or methoxide transfer between these substrates indicating, that unlike the typical solvent-switching reactions for gas-phase adducts, there must be an activation energy involved in releasing a fluoride or methoxide ion from $FGe(OMe)_4^-$, or $FSi(OMe)_4^-$. By comparison, both of these ions can undergo fluoride–methoxide exchange with highly fluorinated species like BF_3 and SO_2F_2 as previously reported [9,12]. These exchange reactions in which the Si and Ge centers retain their pentacoordination are probably activated by the exchange of highly electronegative ligands.

We believe that these gas-phase studies on hypervalent species will continue to provide a valuable insight into the chemistry of the elements of group 14.

Acknowledgements

This work was made possible through the generous support of research grants and a graduate fellowship (LAX) from the São Paulo Science Foundation (FAPESP). NHM and JMR also thank the Brazilian Research Council (CNPq) for support through their Research Fellowship program.

References

[1] C. Chuit, R.J.P. Corriu, C. Reye, J.C. Young, Chem. Rev. 93 (1993) 1371.
[2] (a) M.J. Baerpark, G.S. McGrady, P.D. Prince, J.W. Steed, J. Am. Chem. Soc. 123 (2001) 7736;
(b) A.R. Bassindale, S.G. Glynn, P.G. Taylor, N. Auner, B. Herrschaft, J. Organometal. Chem. 619 (2001) 132;
(c) A.R. Bassindale, M. Borbaruah, S.G. Glynn, D.J. Parker, P.G. Taylor, J. Organometal. Chem. 606 (2000) 125;
(d) S.D. Kincade, J.W. Del Nin, A.S. Schach, T.A. Sloan, K.L. Wilson, C.T.G. Knight, Science 285 (1999) 1542;
(e) A. Kolomeitsev, G. Bissky, E. Lork, V. Movchun, E. Rusanov, P. Kirsch, G.V. Roschenthaler, Chem. Commun. (1999) 1017;
(f) R.J.P. Corriu, C. Guerin, B.J.L. Henner, Q.J. Wang, Organometallics 10 (1991) 3574.
[3] (a) J.R. Chipperfield, R.H. Prince, J. Chem. Soc. (1963) 3567;
(b) A.J. Cleland, S.A. Fieldhouse, B.H. Freeland, R.J. O'Brien, J. Chem. Soc., Chem. Commun. (1971) 155;
(c) P. Riviere, A. Castel, J. Satge, J. Organometal. Chem. 232 (1982) 123;
(d) D.J. Brauer, J. Wilke, R. Eujen, J. Organometal. Chem. 316 (1986) 261.
[4] C.H. DePuy, V.M. Bierbaum, L.A. Flippin, J.J. Grabowski, G.K. King, R.J. Schmitt, S.A. Sullivan, J. Am. Chem. Soc. 102 (1980) 5012.
[5] S.A. Sullivan, C.H. DePuy, R. Damrauer, J. Am. Chem. Soc. 103 (1981) 480.
[6] D.J. Hajdasz, Y. Ho, R.R. Squires, J. Am. Chem. Soc. 116 (1994) 10751.
[7] R. Damrauer, L.W. Burggraf, L.P. Davis, M.S. Gordon, J. Am. Chem. Soc. 110 (1988) 6601.
[8] M.L.P. Silva, J.M. Riveros, J. Mass Spectrom. 30 (1995) 733.
[9] N.H. Morgon, A.B. Argenton, M.L.P. da Silva, J.M. Riveros, J. Am. Chem. Soc. 119 (1997) 1708.
[10] M.L.P. Silva, J.M. Riveros, Int. J. Mass Spectrom. Ion Process. 165/166 (1997) 83.
[11] L.A. Xavier, J.M. Riveros, Int. J. Mass Spectrom. Ion Process. 179/180 (1998) 223.
[12] N.H. Morgon, L.A. Xavier, J.M. Riveros, Int. J. Mass Spectrom. 195/196 (2000) 363.
[13] L.L. Hench, J.K. West, Chem. Rev. 90 (1990) 33.
[14] V. Stanic, T.H. Etsell, A.C. Pierce, R.J. Mikula, J. Mater. Chem. 7 (1997) 105.
[15] R.J.P. Corriu, C. Guérin, B.J.L. Henner, Q. Wang, Organometallics 10 (1991) 3200.
[16] C. Chuit, R.J.P. Corriu, C. Reye, J.C. Young, J. Organometal. Chem. 358 (1988) 57.
[17] D. Schomburg, J. Organometal. Chem. 221 (1981) 137.
[18] S.E. Johnson, J.A. Deiters, R.O. Day, R.R. Holmes, J. Am. Chem. Soc. 111 (1989) 3250.
[19] S.E. Johnson, R.O. Day, R.R. Holmes, Inorg. Chem. 28 (1989) 3182.
[20] D.M. Wetzel, J.I. Brauman, Chem. Rev. 87 (1987) 607.
[21] C.R. Moylan, J.A. Dodd, C.-C. Han, J.I. Brauman, J. Chem. Phys. 86 (1987) 5350.
[22] Y. Yang, H.V. Linnert, J.M. Riveros, K.R. Williams, J.R. Eyler, J. Phys. Chem. A 101 (1997) 2371.
[23] N.H. Morgon, J.M. Riveros, J. Mol. Struct. (Theochem.) 539 (2001) 135.
[24] J.J. Menegon, V. Linnert, Quim. Nova 19 (1996) 423.
[25] T.G. Clements, A.K. Luong, H.-J. Deyeri, R.E. Continetti, J. Chem. Phys. 114 (2001) 8436.
[26] (a) G.L. Gutsev, J. Chem. Phys. 166 (1992) 57;
(b) G.L. Gutsev, J. Chem. Phys. 99 (1993) 3906.

[27] R.A. King, V.S. Mastryukov, H.F. Schaefer III, J. Chem. Phys. 105 (1996) 6880.
[28] E.A. Brinkman, E. Günther, O. Schafer, J.I. Brauman, J. Chem. Phys. 100 (1994) 1840.
[29] C. Blondel, P. Cacciani, C. Delsart, R. Trainham, Phys. Rev. A 40 (1989) 3698.
[30] (a) J.W. Larson, T.B. McMahon, J. Am. Chem. Soc. 107 (1985) 766;
(b) J.W. Larson, T.B. McMahon, Inorg. Chem. 26 (1987) 4018.
[31] (a) T.M. Ramond, G.E. Davico, R.L. Schwartz, W.C. Lineberger, J. Chem. Phys. 112 (2000) 1158;
(b) D.L. Osborn, D.J. Leahy, E.H. Kim, E. de Beer, D.M. Neumark, Chem. Phys. Lett. 292 (1998) 651.
[32] R. Custodio, M. Giordan, N.H. Morgon, J.D. Goddard, Int. J. Quantum Chem. 42 (1992) 411.
[33] R. Custodio, J.D. Goddard, M. Giordan, N.H. Morgon, Can. J. Chem. 70 (1992) 580.
[34] W.J. Stevens, H. Basch, M. Krauss, J. Chem. Phys. 81 (1984) 6026.
[35] N.H. Morgon, J.M. Riveros, J. Phys. Chem. A 102 (1998) 10399.
[36] N.H. Morgon, J. Phys. Chem. A 102 (1998) 2050.
[37] M.J. Frisch, G.W. Trucks, M. Head-Gordon, P.M.W. Gill, M.W. Wong, J.B. Foresman, B.G. Johnson, H.B. Schlegel, M.A. Robb, E.S. Replogle, R. Gomperts, J.L. Andres, K. Raghavachari, J.S. Binkley, C. Gonzalez, R.L. Martin, D.J. Fox, D.J, Defrees, J. Baker, J.J.P. Stewart, J.A. Pople, Gaussian 94, Revision D.2, Gaussian, Inc., Pittsburgh, PA, 1995.
[38] M.S. Gordon, L.P. Davis, L.W. Burgraff, in: N.G. Adams, L.M. Babcock (Eds.), Advances in Gas Phase Ion Chemistry, JAI Press, Greenwich, CT, 1992, p. 203.
[39] N.H. Morgon, J.M. Riveros, Int. J. Mass Spectrom. 210/211 (2001) 173.
[40] Q. Li, G. Li, W. Xu, Y. Xie, H.F. Schaefer III, J. Chem. Phys. 111 (1999) 7945.
[41] K.R. Lykke, K.K. Murray, W.C. Lineberger, Phys. Rev. A 43 (1991) 6104.